

# Numerical Simulation of Geosynthetic Reinforced Embankments

Christian Lackner

*Graz University of Technology, Institute for Soil Mechanics and Foundation Engineering  
Christian.Lackner@tugraz.at*

## ABSTRACT

This paper is dealing with conventional, analytical calculation methods and numerical simulations of geosynthetic reinforced embankments. Two and three-dimensional analysis are performed. For conventional calculations GGU Software is used and for numerical simulations Plaxis V.8 and Plaxis 3D Tunnel is employed. The goal is to simulate respectively to evaluate the behavior of geosynthetic reinforced embankments. The differences between conventional and numerical calculations are shown and the results are compared. An important aspect is the determination of the global safety factor and the failure mechanism. With Plaxis the deformations of the embankment and the resulting forces in geosynthetics and anchors are calculated. Variation of the ground stiffness and the road roller compaction force shows the influence on the forces in geosynthetics and anchors. The settlements of the embankment are calculated and a comparison with measurements at the project Trieben–Sunk is provided. Finally advantages and disadvantages of each, conventional and numerical method of calculation, are shown.

*Keywords: Geosynthetics, Embankment, FEM, Plaxis, Trieben–Sunk*

## INTRODUCTION

More and more geosynthetic reinforced embankments find their acceptance in modern building design as an economic solution. In Trieben–Sunk, Upper Styria, Austria, such a construction is currently in progress. In this area a continuous creeping of the slopes of the valley is measured up to three cm per year. Therefore a “soft” structure that is able to sustain the deformations without stress concentrations is designed. Up to 30 m high, 60° sloped, geosynthetic reinforced embankments are planned to lead the road B 114 from Trieben to Hohentauern.

Conventional analysis is often not sufficient to design such geosynthetic reinforced embankments. Nowadays numerical simulations give a better understanding of the behavior of the construction and the occurring deformations. The aim of the paper is to investigate the behavior of geosynthetic reinforced embankments and to show the differences between conventional analysis and numerical simulation related to such constructions.

## GEOSYNTHETIC REINFORCED EMBANKMENTS

### *Construction Principle*

Henri Vidal in 1960 mentioned in his PhD thesis reinforced embankments with steel bands. In 1980, geosynthetics were implemented to absorb the ground's tension.

Close to the principle of reinforced concrete, soil is only able to sustain little tension. With increasing the shear strength in a not reinforced soil up to failure, movements in the shear zone occur. Because of the tension strength of the geosynthetic and the friction between soil and the geosynthetic the movement can be stopped and equilibrium can be reached.

### Classification

Tab.1 shows a classification of geosynthetics.

Table 1. Classification of geosynthetic

permeable to water		impermeable to water	
Geotextile	Geotextile related product ( <b>geogrids</b> )	Liner sheet	Liner sheet related product

In Trieben–Sunk geotextile related products, so called geogrids are used to reinforce the designed embankments.

### Embankment construction

The construction sequence of a geogrid reinforced embankment is shown in Fig.1.

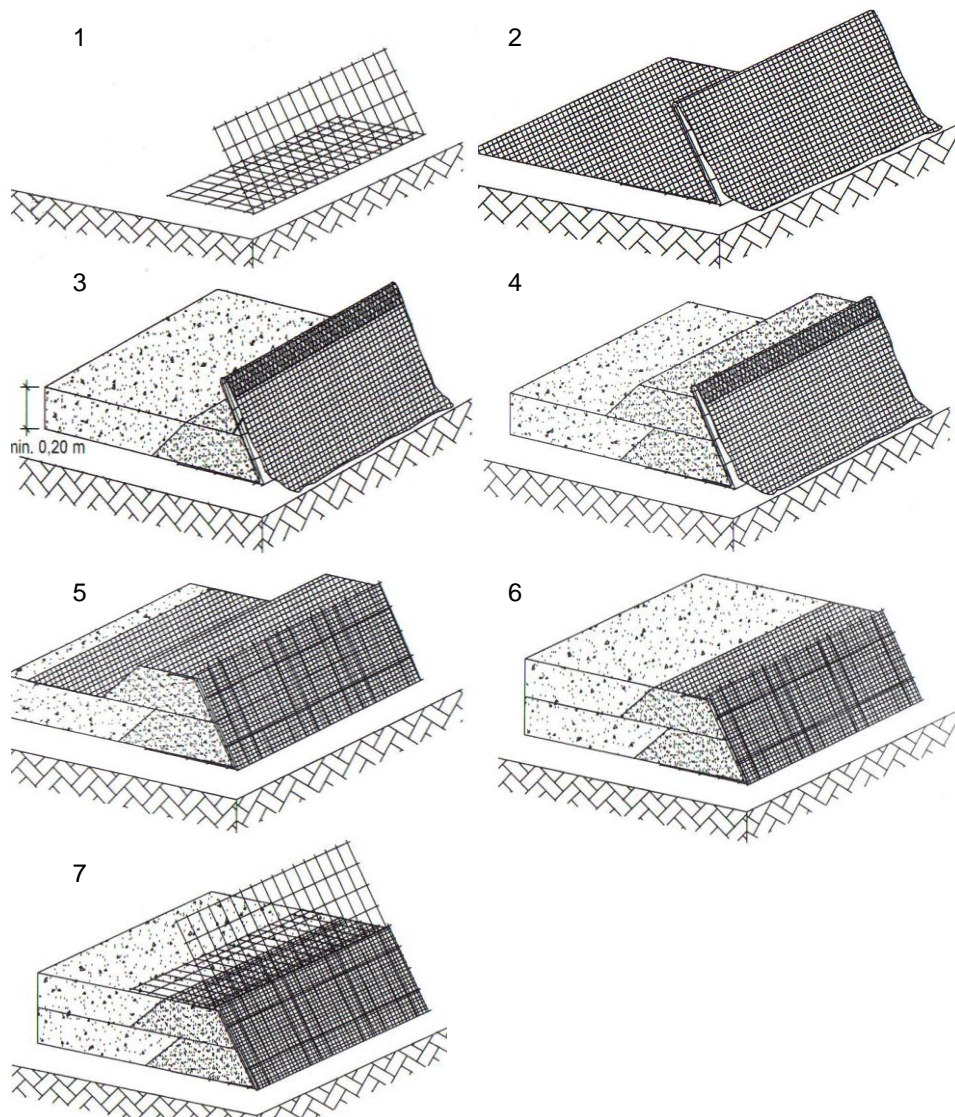


Figure 1. Embankment construction

## PROJEKT TRIEBEN - SUNK

### *General project information*

The "B114 Triebener Bundesstraße" is an important connection between highway A9 in Upper and the motorway S36 in Lower Styria. On the average 2000 vehicles per day pass the road, nine percent trucks are counted. During construction of the new B114 the daily traffic flow must not be handicapped. Therefore, the new road was planned on the opposite side of the valley in "Wolfsgraben". Date 06.06.2006 was defined for the commencement of construction. In October 2008 the approval for traffic shall be given. In June 2009 the whole construction shall be finished. The building costs are calculated with about 21 million Euro.

### *Geotechnical project information*

The 2,9 km long road is divided in seven geotechnical zones. This paper is dealing with zone three, the geologically most endangered area. A geological cross section for profile 46 in geotechnical zone three is shown in Fig.2. Geologically the cross section is composed of coarse grain dominated slope debris (1), which is interrupted by aquiferous fine grain dominated slope debris (2). The constructive design of the geosynthetic reinforced embankment and the stabilising procedures are shown in Fig.3. Shotcrete and 12 m long IBO anchors, are used to cover the excavation due to the embankment's footing. A reinforced concrete plate is planned to foot the embankment. To prevent a slip failure two 16 m long GEWI anchors are installed. The construction sequence of the geosynthetic reinforced embankment is explained in chapter geosynthetic reinforced embankments.

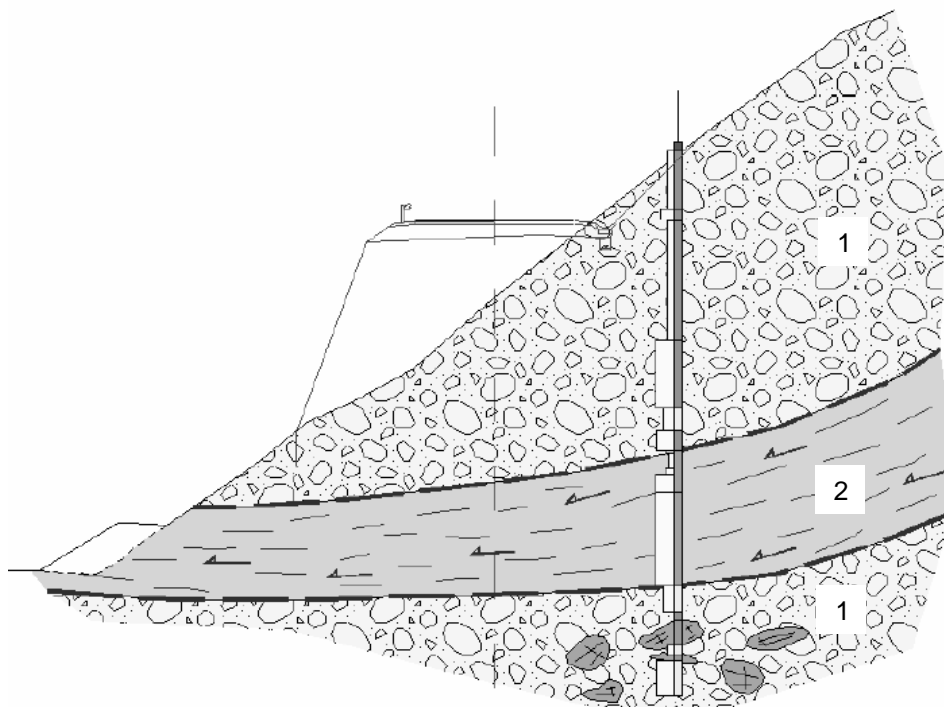


Figure 2. Geological cross section (3G Gruppe Geotechnik Graz ZT GmbH)

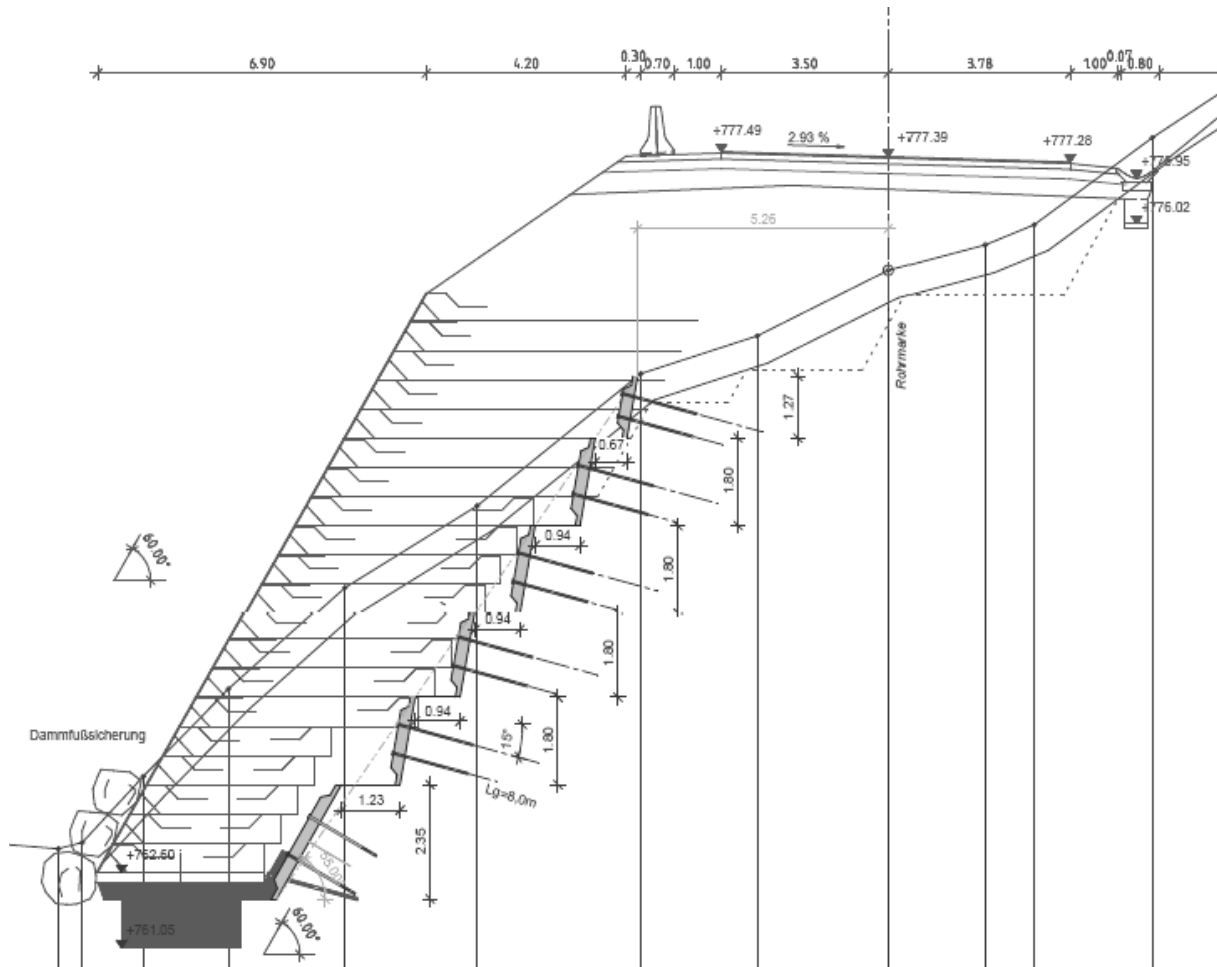


Figure 3. Cross section of the slope with support measures and embankment (ZT Büro Dr. Karl Lackner)

## CONVENTIONAL ANALYSIS

### *Conventional approaches*

For conventional analysis two approaches, Bishop and Janbu, after DIN 4084 are used. To make the comparison between conventional analysis and numerical simulation possible, the factor of safety is calculated as a global factor.

### *Calculation*

The model for conventional analysis is based on the geological and constructive cross section shown in Fig.2 and Fig.3. Four calculations are performed. In the first analysis, the factor of safety for the inventory slope is determined. In addition an analysis for the construction step, excavation, covering with shotcrete and anchoring the slope is performed. In the next step, calculation three, the geosynthetic reinforced embankment is implemented and the global safety factor again is estimated. Finally, the embankment's safety itself is determined.

The inner safety is specified by the long-time tensile strength of the geogrid. The long-time tensile strength is calculated with equ.(1)

$$z_{Rd} = \frac{r}{A_1 * A_2 * A_3 * A_4 * \gamma} \quad [kN/m] \quad (1)$$

- $z_{Rd}$ ... Minimal value of long time tensile strength
- $r$ ... Minimal value for short time tensile strength
- $A_1$ ... Reduction ratio concerning creeping
- $A_2$ ... Reduction ratio concerning damage (transport, compaction)
- $A_3$ ... Reduction ratio concerning converting
- $A_4$ ... Reduction ratio concerning environmental conditions
- $\gamma$ ... Material safety factor

**Results**

The results of the conventional analysis are given in Tab.2.

Table 2. Global factor of safety of conventional analysis Bishop/Janbu

Inventory slope	Excavation	Embankment	Inner stability
1,21/1,18	1,32/1,29	1,33/1,28	1,84/1,78

The failure mechanism of the different construction steps, inventory slope, excavation, embankment and inner stability are shown in Fig.4.

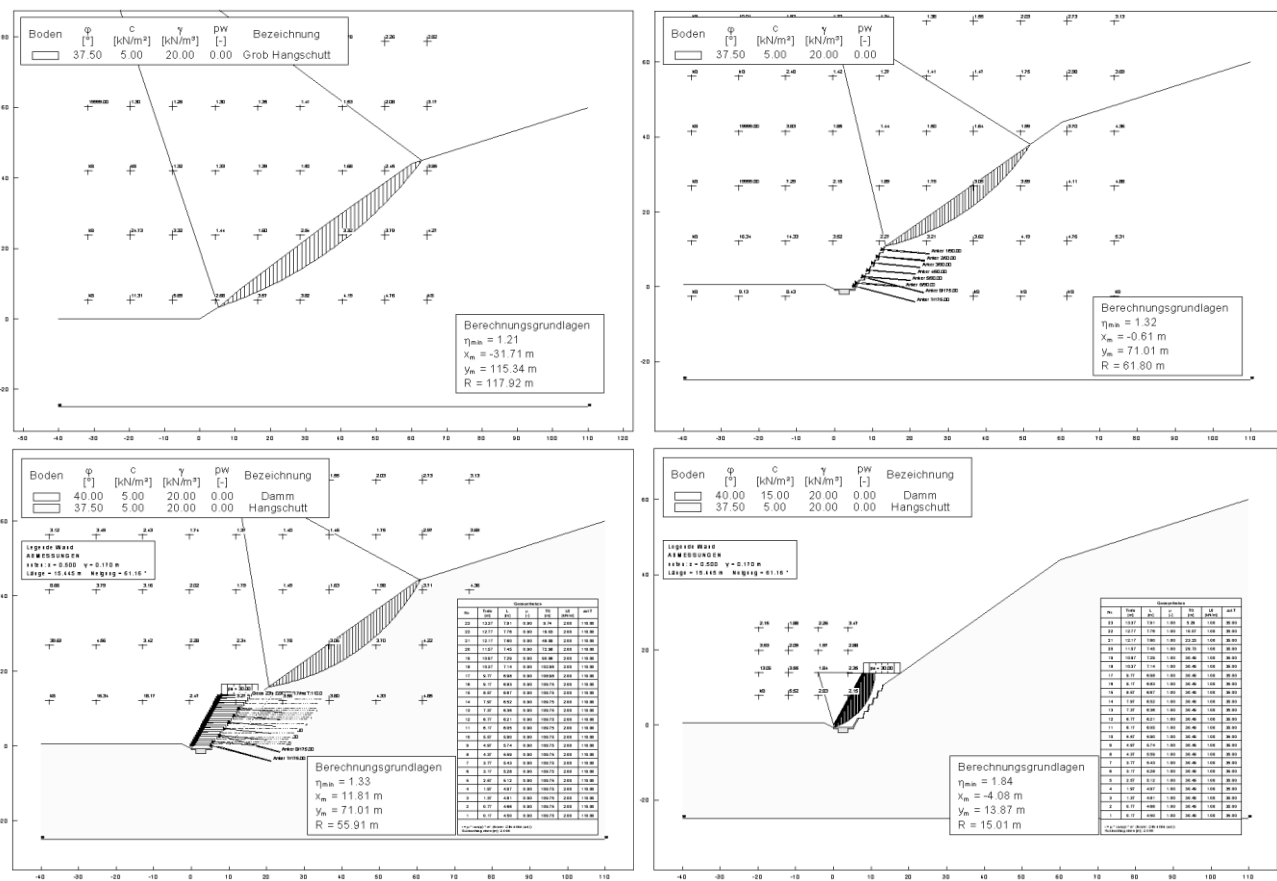


Figure 4. Failure mechanism (GGU Stability)

**NUMERICAL SIMULATION**

The numerical simulations include the calculation of the factor of safety by phi-c reduction, the forces in geogrids and anchors and the deformation of the embankment during the construction process.

**Calibration**

In addition the numerical simulation is calibrated related to the factor of safety, see Fig.5. Three-dimensional effects are also implemented in the two-dimensional model, see Fig.6. A comparison between the maximum expanse of excavation in 3D, shortly before failure, and the maximum percentage of excavation in 2D ( $m_{stage}$ ) is drawn.

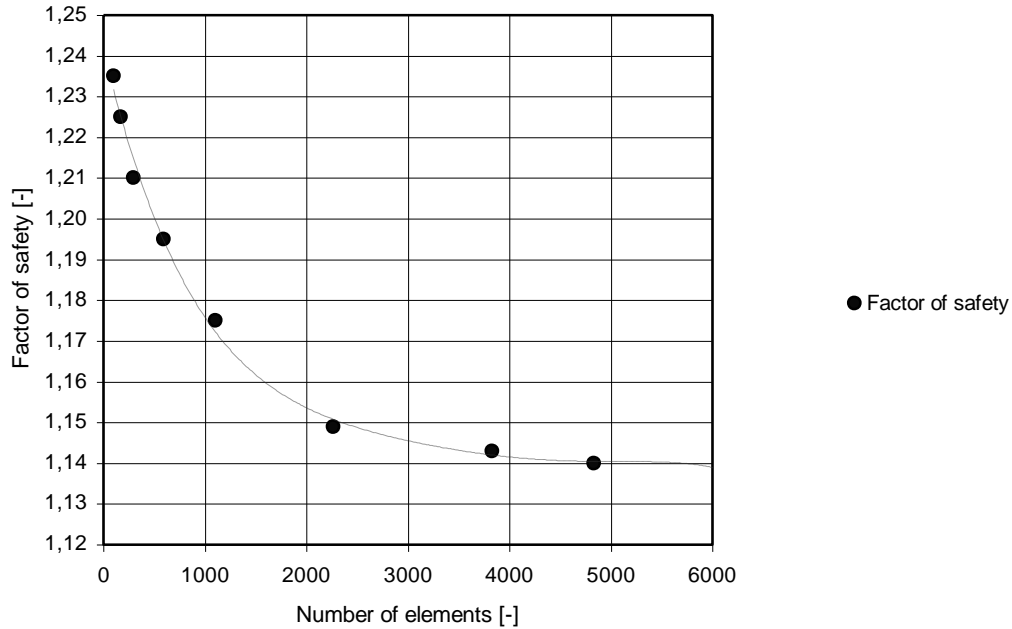


Figure 5. Number of elements vs. factor of safety.

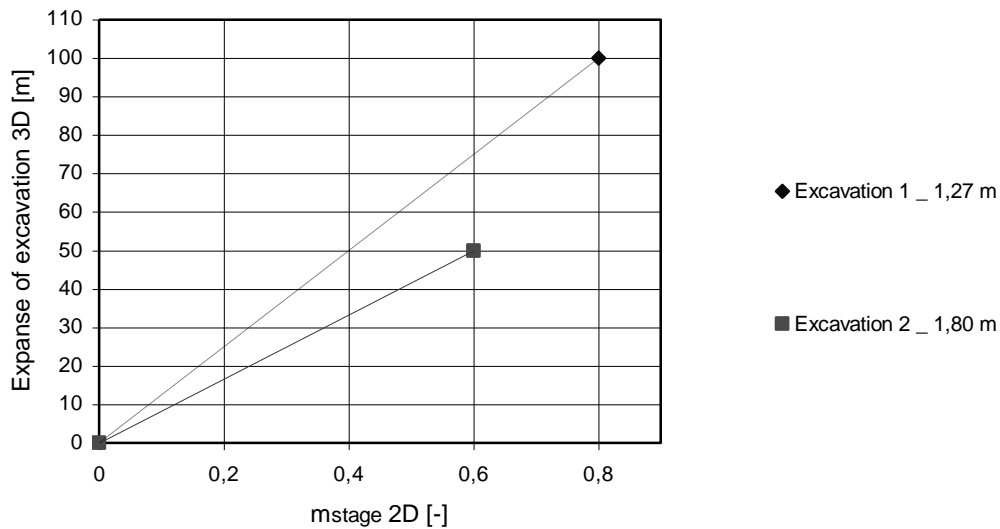


Figure 6.  $m_{stage}$  2D vs. expanse of excavation 3D

Therefore the calibrated two-dimensional model runs with 4015 elements and the  $m_{stage}$  of 0,4 is implemented in the calculation to simulate the finite, uncovered excavation in 3D.

## Results

The results for the factor of safety are given in Tab.3 and the numerical failure mechanism is shown in Fig.7.

Table 3. Global factor of safety of the numerical simulation with Plaxis V8 2D

Inventory slope	Excavation	Embankment	Inner stability
1,14	1,21	1,22	1,72

The calculated forces in the geogrids are shown in Fig.8 and Fig.9. The maximum force in the geogrids amounts to 15,5 kN/m and is dependent on the ground stiffness (Fig.8) and the road roller's compaction force (Fig.9).

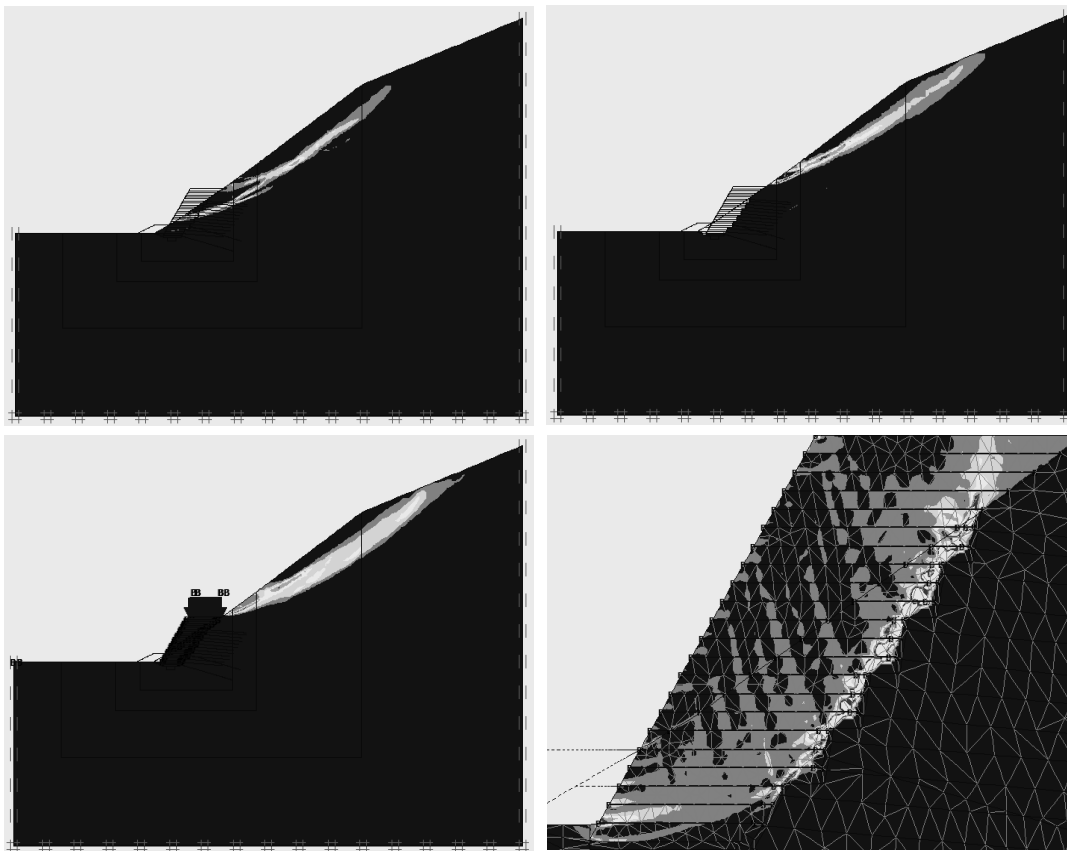


Figure 7. Failure mechanism (shear shadings)

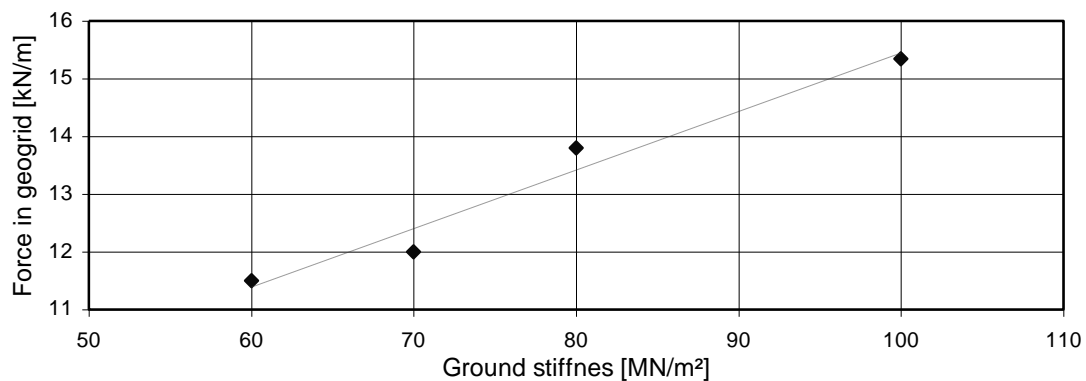


Figure 8. Ground stiffness vs. tensile force in geogrid

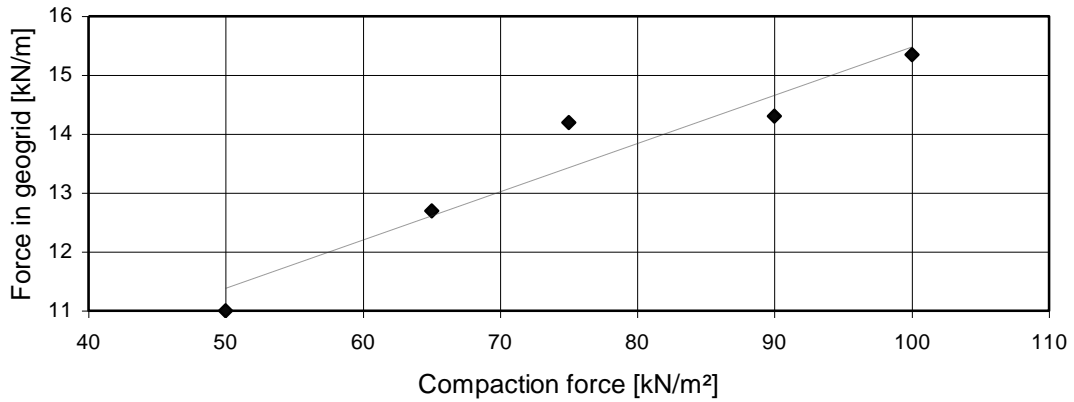


Figure 9. Compaction force vs. tensile force in geogrid

The forces in the IBO and GEWI – anchors are shown in Fig.10 and Fig.11. The amount of the maximum IBO anchor force is 55 kN/m, the GEWI anchor's maximum force amounts nearly to 105 kN/m. The results are presented including a variation of the ground stiffness (Fig.10) and the compaction force (Fig.11).

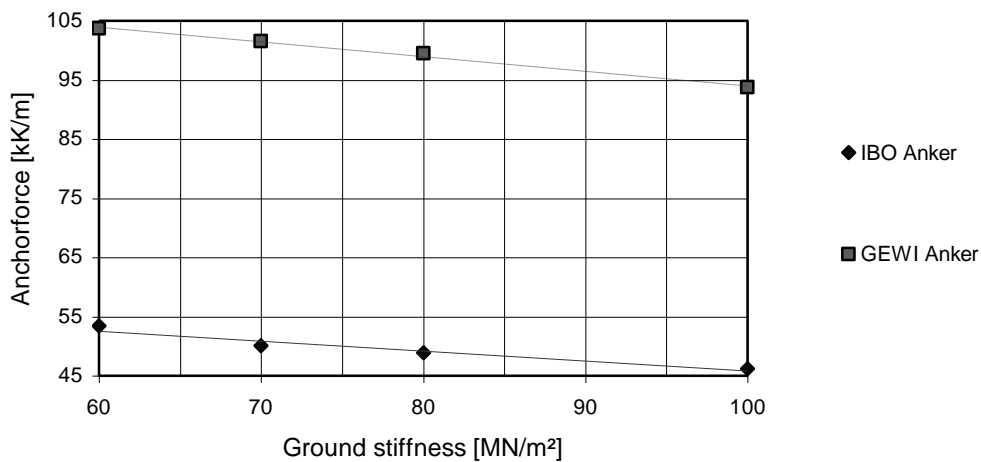


Figure 10. Ground stiffness vs. tensile force in anchor

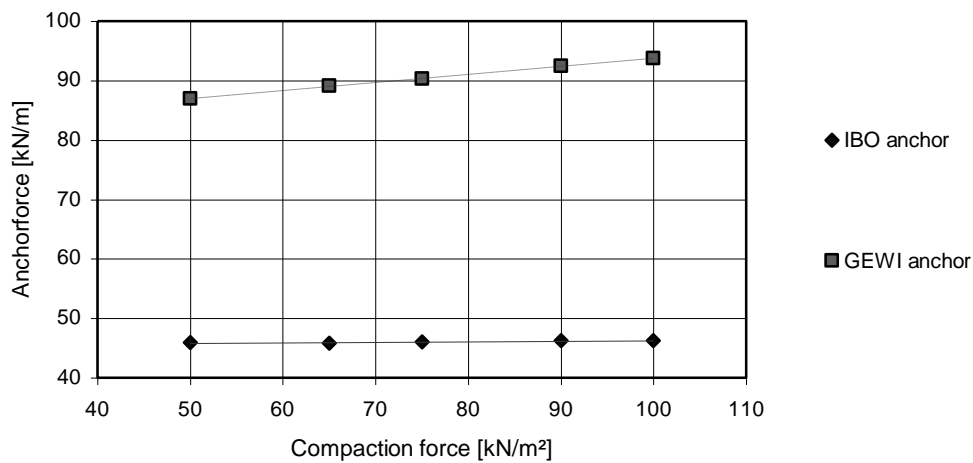


Figure 11. Compaction force vs. tensile force in anchor

Additionally the deformations of the embankment during the construction process are calculated and presented in Fig.12. In the last calculation step, activating traffic load on the finished embankment, the maximum settlements amount to 10,4 cm. After excavating the slope until foundation (small picture Fig.12) a heaving up to 2,2 cm occurs. Therefore, total settlements from 12,6 cm can be calculated Fig.12. 13 cm loss of cubature is measured for a 13 m high embankment at the building site.

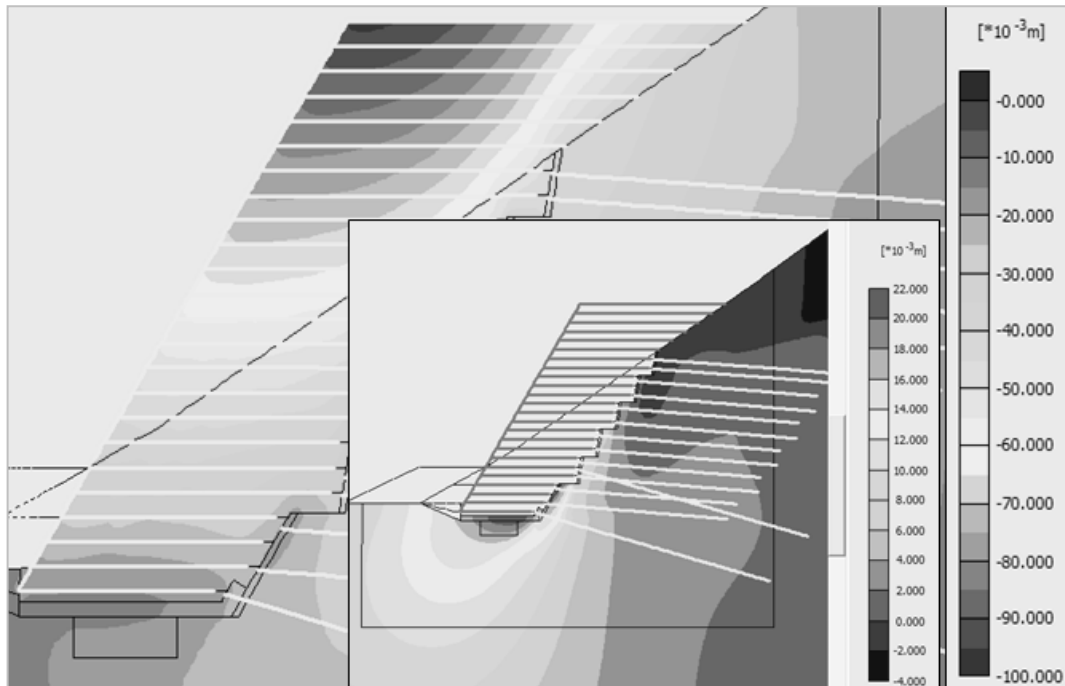


Figure 12. Total vertical displacements of the geosynthetic reinforced embankment

## SUMMARY AND OUTLOOK

The comparison of the analytically calculated factors of safety and those from the  $\phi$ - $c$  reduction of the numerical simulation shows related results (Tab.2 and Tab.3). The failure mechanism is also comparable, see Fig. 4 and Fig. 7, although, Plaxis V8 2D itself detects the more critical failure function, which can be seen in the lower factor of safety.

The time economy of the conventional analysis faces the flexibility of numerical simulations. In one single simulation, it is possible to calculate on the one hand the factor of safety (Ultimate Limit State) and on the other hand the deformations of the embankment (Serviceability Limit State) including the resulting forces in geogrids and anchors.

In every case, modeling a numerical simulation of a geosynthetic reinforced embankment is essential to get a deeper insight into the behavior of the interaction between embankment and geogrid.

## REFERENCES

- prEN, 2000. Geokunststoffe und ihre Definition. Europäischer Normenausschuss*
- DIN 4084, 2002. Baugrund – Geländebruchberechnungen. Beuth Verlag.*
- Schweizer Verband für Geokunststoffe, 2003. Bauen mit Geokunststoffen. SVG.*
- Ulrich Smolczyk, 2001. Grundbautaschenbuch-Bauverfahren. Ernst und Sohn.*
- Brinkgreve R.B.J & Technische Universität Delft & PLAXIS, 2003. Plaxis V8 Manual. A.A. Balkema Publishers*
- GGU Zentrale Verwaltung mbH, 2006. GGU – Stability. GGU Zentrale Verwaltung mbH, Braunschweig*
- Gruppe Geotechnik Graz ZT GmbH, 2005. Gutachten zur Geologie und Geotechnik. (unpublished)*
- Lackner, K., 2005. Technischer Bericht zur Bodenmechanischen und Geotechnischen Gutachtertätigkeit während der Planungsphase. (unpublished)*